Journal of Photochemistry and Photobiology A: Chemistry 210 (2010) 125–129

Contents lists available at ScienceDirect

Journal of Photochemistry and Photobiology A: Chemistry

journal homepage: www.elsevier.com/locate/jphotochem

Thermally induced phase and photocatalytic activity evolution of polymorphous titania

N. Mahdjoub, N. Allen*, P. Kelly, V. Vishnyakov

Dalton Research Institute, Manchester Metropolitan University, Manchester M1 5GD, UK

ARTICLE INFO

Article history:
Received 29 October 2009
Received in revised form 5 January 2010
Accepted 8 January 2010
Available online 18 January 2010

Keywords:
Titanium dioxide
Photocatalysis
Anatase
Brookite
Rutile

ABSTRACT

TiO_2 nano-powders were prepared by hydrolysing titanium tetraisopropoxide at room temperature. The resulting products were dried at 382 K and then annealed at temperatures up to 1172 K for 1 h. Raman analysis showed different titania phase structures depending on the thermal treatment. A mixture of brookite and anatase was observed in the as-prepared sample and after thermal treatment at 472 K and 672 K, a mixture of anatase and rutile was observed at 872 K and 972 K, while a pure rutile phase was identified at 1172 K. Quantitative XRD analysis revealed nano-powders phase composition and crystallite sizes. The photoactivity was assessed by photoinduced degradation of methyl orange. All anatase–brookite compositions have showed high photoactivity while the best values were observed for the sample calcined at 472 K.

1. Introduction

Titanium dioxide is very widely used in applications such as photocatalysis to remove pollutants from air and water, deodorizing, solar cells and as a luminescent material [1–4]. Titania can be extracted from minerals or created from solutions of titanium salts or alkoxides through one of many possible well known routes such as the sulphate process, the chloride process, the hydrothermal method or the sol–gel process [5–7]. TiO_2 is a polymorphic material, which exists in few crystallographic forms such as tetragonal rutile and anatase, or orthorhombic brookite. In rutile, two opposing edges of an octahedron are shared to form linear chains along the edge direction, and the TiO_6 chains are linked to each other via corner connections. Anatase has no edge sharing, but has four corners shared per octahedron. The crystal structure of anatase, which is tetragonal, can be viewed as zigzag chains of the octahedra linked together through corner sharing. In brookite, on the other hand, the octahedral share both edges and corners, forming an orthorhombic structure [8,9].

Anatase and brookite are thermodynamically metastable to rutile. As it happens, anatase and rutile are very common and have been studied in more detail than brookite. Anatase is the phase normally found in the sol–gel syntheses of TiO_2, but brookite is often observed as a by-product. Pure brookite without rutile or anatase is rather difficult to prepare [4,10–13].

Many papers are concerned with the photocatalytic application of TiO_2 and it is generally accepted that anatase is more efficient as a photocatalyst than rutile and brookite. Rutile has rarely been found to be active for the photodegradation of organic compounds in aqueous solutions by itself but good levels of photoactivity have been shown by samples containing mixtures of anatase and rutile. Brookite has been far less studied and characterised compared to anatase or rutile, due to the difficulties observed in making pure brookite. Nevertheless, some kinetics of the transformation of brookite to rutile have been partially been investigated [14–16]. This is despite the fact that there is evidence to indicate that brookite nanocrystals possess excellent photocatalytic capacities for dehydrogenation of 2-propanol [4,13]. The current study aimed to investigate mixed phases of anatase–brookite and their evolution during calcination in air, and, also, to establish photoactivity of investigated polymorphs.

2. Experimental

2.1. Titania nano-powder preparation

For the present study mixed phases of brookite and anatase have been synthesised. The materials, in nano-powder form, were prepared by hydrolysing titanium tetraisopropoxide at room temperature in a process where the isopropoxide is added drop-wise to demineralised water. The resulting precipitate was then filtered, washed and dried at 382 K. Some samples later were calcinated

* Corresponding author at: Manchester Metropolitan University, Chemistry and Materials, Chester St., Manchester, UK. Tel.: +44 0161 247 1432; fax: +44 0161 247 6357.
E-mail address: n.S.allen@mmu.ac.uk (N. Allen).

1010-6030/$ – see front matter © 2010 Elsevier B.V. All rights reserved.
doi:10.1016/j.jphotochem.2010.01.007

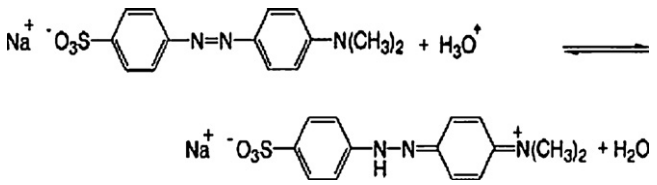

Fig. 1. Structure formula of methyl orange.

(thermally treated) in an open air furnace at various temperatures for 1 h in each case.

2.2. Material characterisation

The titania samples were characterised by XRD and micro-Raman spectroscopy. XRD spectra were scanned over the range 15–100° in 2θ configuration utilising copper radiation. The measured diffraction patterns were inspected against TiO_2 phase reference spectra (rutile, anatase and brookite). Reference patterns are deleted for those phases that do not appear to be present. The reference patterns include crystallographic data which is then used in the Rietveld refinement of the pattern. During this process the software attempts to refine the combined theoretical pattern so that it matches the experimental pattern. This is done by changing various parameters. These parameters can be global (such as the background fit) or phase specific (scale, peak shape, unit cell dimensions, etc). Quantitative data is generated by the software – the accuracy of this is dependent upon the integrity of the fit.

Nano-crystallite sizes were estimated from the broadening of diffraction peaks by the use of Scherrer's equation:

$$D = \frac{k\lambda}{\beta \cos\theta}$$

where D is the grain size, k is a constant (shape factor), λ is the X-ray wavelength, β is the full width at half maximum of a characteristic diffraction peak and θ is the diffraction angle.

Micro-Raman analysis was carried out using an Invia-Microscope from Renishaw. Spectra were taken from each sample in 5–6 places and the results were averaged after having repeated several times the analysis. The spectra were taken at room temperature with a 514 nm laser.

2.3. Reagents and photocatalysis mechanism

The measurements of photocatalytic activity were based on the degradation of the methyl orange (MeO) reagent. Methyl orange (MeO) analytical grade (100%) purity from Aesar Alfa was used as a simple model of a series of common azo-dyes largely used in the industry. This material is known as an acid–base indicator, orange in base medium and red in acidic medium. Its structure is characterised by sulphonic acid groups, known to be responsible for the high solubility of these dyes in water, which is presented in Fig. 1.

Table 1
Raman peak position (cm^{-1}) for bulk titania phases [17–19].

Brookite	Anatase	Rutile
128(s)		
135(w)		143(w) B_{1g}
	144(vs) E_g	
153(vs)		
172(sh)		
	197(w) E_g	
214(w)		
235(m) c		
247(m)		
		273(sh)
288(w)		
	320(vs) c	320(w)
322(w)		
		357(w)
366(w)		
396(sh)		
	399(s) B_{1g}	
412(w)		
		447(s) E_g
454(w)		
461(w)		
502(w)		
	515(m) A_{1g}	
		519(m) B_{1g}
545(w)		
585(w)		
		612(s) A_{1g}
636(s)	639(m) E_g	
	695(w) B_{1g}	
		826(w) B_{2g}
		950(sh)

vs, very strong; s, strong; m, medium; w, weak; sh, shoulder band; c, combination.

When it is dissolved in distilled water, the MeO UV–vis spectrum showed two absorption maxima (see, for example, Fig. 3). The first band is observed at approximately 270 nm and the second, much more intense band is observed at approximately 458 nm. Changes in these reference bands were used to monitor the photocatalytic degradation of MeO by the nano-powders catalysts. Experiments were carried out at room temperature in a static batch photoreactor consisting of a pyrex cylindrical flask open to air. The use of a magnetic stirrer ensured oxygenation from atmospheric air and a satisfactory mixing of the solution with the nano-powders. The irradiation of the mixture was performed by using artificial UV–vis light source emitting at a wavelength of 365 nm (the instrument used was a "Rank Aldis Tutor 2").

0.1 L of the reacting mixture was prepared by adding 0.3 g of TiO_2 catalysts into distilled water containing some amount (1 mL) of MeO (0.06 M). The mixture was stirred and irradiated for 3 h; samples of 5 mL were then withdrawn from the reactor every 30 min and separated from the TiO_2 particles using filtering syringe. The MeO removal of the dye solution was determined by measuring the absorbance value at 458 nm, using a UV–vis spectrophotometer calibrated in accordance with the Beer–Lambert's law. [1,2].

Table 2
Phase composition and crystallite sizes of samples according to XRD data.

Temperature of calcinations (K)	Anatase presence (%)	Anatase crystallite size (nm)	Brookite presence (%)	Brookite crystallite size (nm)	Rutile presence (%)	Rutile crystallite size (nm)
As-prepared	50.3	5.3	37.8	3.4	Not present	Not present
472 K	58.2	5.7	41.8	3.5	Not present	Not present
672 K	68.7	8.3	31.3	6.2	Not present	Not present
872 K	80.5	24.5	15.1	19.8	4.4	40.9
972 K	5.4	60.1	Not present	Not present	94.6	199
1172 K	Not present	Not present	Not present	Not present	100	498.8

3. Results and discussion

3.1. Characterisation

For convenience the main Raman vibration modes for three titania phases of bulk material from published sources are summarised in Table 1. The Raman spectra for nano-powders are presented in Fig. 2 and quantified results of XRD measurements are presented in Table 2. Both techniques show a similar trend, in that a mixture of brookite and anatase observed in the as-prepared sample persists with thermal treatment up to 872 K where the three main phases of TiO_2 are present. The maximum brookite presence is reached after thermal treatment at 472 K and the maximum anatase presence is reached at 672 K. After 872 K the brookite phase disappears and a mixture of anatase and rutile was observed until further thermal treatment results in the disappearance of the anatase phase at

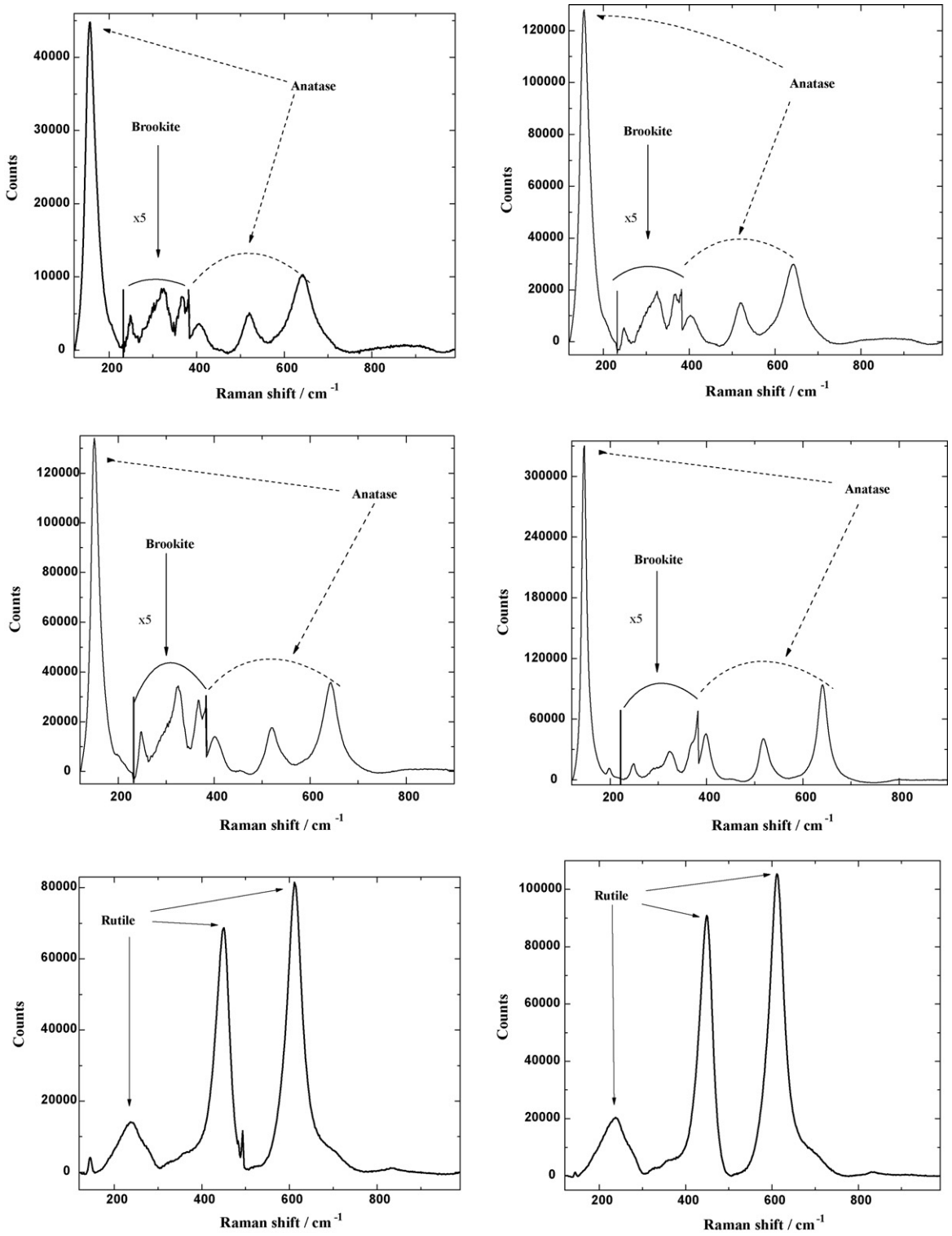

Fig. 2. Raman spectrum of the TiO_2 nano-powders samples (a) as-prepared and thermally treated at elevated temperatures (b) 472 K, (c) 672 K, (d) 872 K, (e) 972 K and (f) 1172 K.

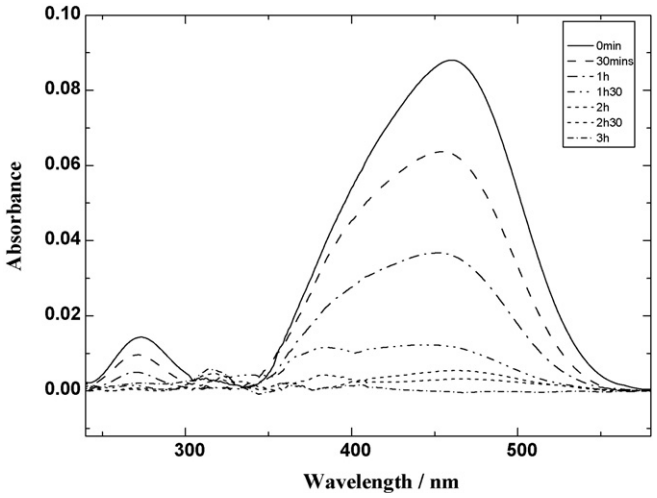

Fig. 3. Optical absorption of methyl orange solution after light irradiations with the titania nano-powder calcinated at 472 K.

1097 K. The TiO_2 samples were then annealed at 1172 K to ensure a full transformation to a thermodynamically more stable rutile phase.

Raman spectra also show effect of phonon confinement on the position of main peaks. Most noticeably this affects main E_g peak for anatase in the 150 cm^{-1} region. For as-prepared sample it is positioned at 157 cm^{-1} which is 13 cm^{-1} shift as compared to the bulk anatase sample. However following calcinations and nano-crystallites growth it shifts to 145 cm^{-1} after treatment at 972 K.

3.2. Photocatalytic assessment

The photocatalytic test, consisting of the degradation of methyl orange, showed a particularly high activity for the samples containing a mixture of anatase and brookite. An example of optical absorption spectra showing degradation of methyl orange during irradiation is presented in Fig. 3. The sample annealed at 472 K consisted of a mixture of approximately 60% anatase and 40% brookite and the sample thermally treated at 672 K is a mixture of approximately 70% anatase and 30% brookite (see Table 2).

Fig. 4 represents the normalised MeO concentration (%) as a function of irradiation time, for all investigated samples. As can be seen all samples with anatase–brookite mixture show high catalytical activity. At the same time sample annealed at 472 K, which had the highest percentage of presence of brookite, also had the highest rate of methyl orange degradation. Moreover, the sample calcined at 472 K almost totally degraded the methyl orange after 180 min of exposure time.

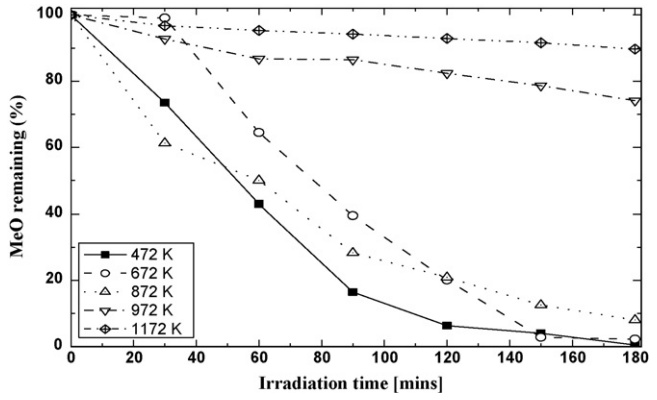

Fig. 4. Reduction of absorption at 472 nm for solutions with nano-powders calcinated at different temperatures.

All the samples selected for investigation showed some degree of photoactivity, except for the sample annealed at 1172 K, which was a pure rutile phase. The sample annealed at 872 K, containing a mixture of anatase/brookite/rutile, showed a high level of activity too, but the sample treated at 972 K, containing approximately 95% rutile, was poorly active. Crystallite size estimates from XRD measurements revealed thermally related grain growth of the particles, as would be expected. This would also be expected to influence activity as larger grain sizes lead to lower surface areas for reactions to occur at. The fact that after almost fivefold incensement in grain size, from the as-prepared sample to the calcinations temperature of 972 K, reduces the activity not so significantly shows that in fact material itself after calcinations at 972 K is probably more active but this activity is hindered by the reduction of surface area. The fact of high activity after calcinations at 972 K can be understood on the basis of improvement of carrier mobility after material annealing.

4. Conclusion

Titania samples rich in brookite were prepared by hydrolysing titanium tetraisopropoxide at room temperature. Samples were thermally treated at different annealing temperatures and key steps were identified due to the presence of brookite phases, anatase phases and rutile phases, either as two or three phase mixtures or as a pure phase. Raman investigations were carried out in order to establish a link between annealing temperature and the phases present. XRD analysis also supported the whole investigation. Assessment of the photocatalytic degradation of methyl orange under UV light showed the high activity of the mixed phase brookite and anatase samples persisting until a key temperature of 872 K, where a three phase structure was observed in the sample. This investigation opened a new set of experiments which could lead to more detailed studies around the brookite phase and other mixtures of the TiO_2 polymorph.

References

[1] N. Guettaï, H. Ait Amar, Photocatalytic oxidation of methyl orange in presence of titanium dioxide in aqueous suspension. Part I: parametric study, Desalination 185 (1–3) (2005) 427–437.
[2] Y. Badr, M.A. Mahmoud, Photocatalytic degradation of methyl orange by gold silver nano-core/silica nano-shell, Journal of Physics and Chemistry of Solids 68 (3) (2007) 413–419.
[3] P.A. Christensen, T.P. Curtis, T.A. Egerton, S.A.M. Kosa, J.R. Tinlin, Photoelectrocatalytic and photocatalytic disinfection of *E. coli* suspensions by titanium dioxide, Applied Catalysis B: Environmental 41 (2003) 371–386.
[4] L. Di Paola, A. Addamo, M. Bellardita, M. Cazzanelli, E. Palmisano, Preparation of photocatalytic brookite thin films, Thin Solid Films 515 (7–8) (2007) 3527–3529.
[5] B. Guo, Z. Liu, L. Hong, H. Jiang, Sol gel derived photocatalytic porous TiO_2 thin films, Surface and Coatings Technology 198 (1–3) (2005) 24–29.
[6] Z. Liu, X. Zhang, T. Murakami, A. Fujishima, Sol–gel SiO_2/TiO_2 bilayer films with self-cleaning and antireflection properties, Solar Energy Materials and Solar Cells 92 (11) (2008) 1434–1438.
[7] S. Boujday, F. Wunsch, P. Portes, J.F. Bocquet, C. Colbeau-Justin, Photocatalytic and electronic properties of TiO_2 powders elaborated by sol–gel and supercritical drying, Solar Energy Materials and Solar Cells. 83 (2004) 421–433.
[8] M. Diebold, The Causes and Prevention of TiO_2 Photodegradation of Paints, Dupont Company, 1995.
[9] N. Martin, C. Rousselot, D. Rondot, F. Palmino, R. Mercier, Microstructure modification of amorphous titanium oxide thin films during annealing treatment, Thin Solid Films 300 (1997) 113–121.
[10] T. Ozawa, M. Iwasaki, H. Tada, T. Akita, K. Tanaka, S. Ito, Low-temperature synthesis of anatase–brookite composite nanocrystals: the junction effect on photocatalytic activity, Journal of Colloid and Interface Science 281 (2) (2005) 510–513.
[11] W. Luo, S.F. Yang, Z.C. Wang, Y. Wang, R. Ahuja, B. Johansson, J. Liu, G.T. Zou, Structural phase transitions in brookite-type TiO_2 under high pressure, Solid State Communications 133 (1) (2005) 49–53.

[12] I.N. Kuznetsova, V. Blaskov, I. Stambolova, L. Znaidi, A. Kanaev, TiO_2 pure phase brookite with preferred orientation, synthesized as a spin-coated film, Materials Letters 59 (29–30) (2005) 3820–3823.
[13] A. Di Paola, G. Cufalo, M. Addamo, M. Bellardita, R. Campostrini, M. Ischia, R. Ceccato, L. Palmisano, Photocatalytic activity of nanocrystalline TiO_2 (brookite, rutile and brookite-based) powders prepared by thermohydrolysis of $TiCl_4$ in aqueous chloride solutions, Colloids and Surfaces A: Physicochemical and Engineering Aspects 317 (1–3) (2008) 366–376.
[14] R. Zallen, M.P. Moret, The optical absorption edge of brookite TiO_2, Solid State Communications 137 (3) (2006) 154–157.
[15] M.P. Moret, R. Zallen, D.P. Vijay, S.B. Desu, Brookite-rich titania films made by pulsed laser deposition, Thin Solid Films 366 (1–2) (2000) 8–10.
[16] X. Bokhimi, F. Pedraza, Characterization of brookite and a new corundum-like titania phase synthesized under hydrothermal conditions, Journal of Solid State Chemistry 177 (7) (2004) 2456–2463.
[17] J.-G. Li, T. Ishigaki, Brookite → rutile phase transformation of TiO_2 studied with monodispersed particles, Acta Materialia 52 (17) (2004) 5143–5150.
[18] I.M. Arabatzis, T. Stergiopoulos, M.C. Bernard, D. Labou, S.G. Neophytides, P. Falaras, Silver-modified titanium dioxide thin films for efficient photodegradation of methyl orange, Applied Catalysis B: Environmental 42 (2) (2003) 187–201.
[19] Y. Yu, J.C. Yu, J.-G. Yu, Y.-C. Kwok, Y.-K. Che, J.-C. Zhao, L. Ding, W.-K. Ge, P.-K. Wong, Enhancement of photocatalytic activity of mesoporous TiO_2 by using carbon nanotubes, Applied Catalysis A: General 289 (2) (2005) 186–196.